

## RESEARCH LETTER

10.1002/2017GL075900

## Key Points:

- The Southwest Madagascar Coastal Current (SMACC) is a newly discovered surface poleward current
- The SMACC exhibits a seasonal cycle and is driven by the wind stress curl
- The SMACC influences the coastal upwelling region south of Madagascar

## Supporting Information:

- Supporting Information S1
- Figure S1
- Figure S2
- Figure S3
- Figure S4
- Data Set S1

## Correspondence to:

J. D. Ramanantsoa,  
oceanman1@live.fr

## Citation:

Ramanantsoa, J. D., Penven, P., Krug, M., Gula, J., & Rouault, M. (2018). Uncovering a new current: The Southwest Madagascar Coastal Current. *Geophysical Research Letters*, 45, 1930–1938. <https://doi.org/10.1002/2017GL075900>






Received 2 OCT 2017

Accepted 21 JAN 2018

Accepted article online 25 JAN 2018

Published online 22 FEB 2018

## Uncovering a New Current: The Southwest Madagascar Coastal Current

Juliano D. Ramanantsoa<sup>1,2,3</sup> , P. Penven<sup>4</sup> , M. Krug<sup>1,2,5</sup> , J. Gula<sup>4</sup> , and M. Rouault<sup>1,2</sup> 

<sup>1</sup>Department of Oceanography, University of Cape Town, Cape Town, South Africa, <sup>2</sup>Nansen Tutu for Marine Environmental Research, Ma-Re Institute, University of Cape Town, Cape Town, South Africa, <sup>3</sup>Institut Halieutique et des Sciences Marines, Toliara, Madagascar, <sup>4</sup>University Brest, CNRS, IRD, Ifremer, Laboratoire d'Océanographie Physique et Spatiale, IUEM, Brest, France, <sup>5</sup>Council for Scientific and Industrial Research, Cape Town, South Africa

**Abstract** Cruise data sets, satellite remote sensing observations, and model data analyses are combined to highlight the existence of a coastal surface poleward flow in the southwest of Madagascar: the Southwest Madagascar Coastal Current (SMACC). The SMACC is a relatively shallow (<300 m) and narrow (<100 km wide) warm and salty coastal surface current, which flows along the south western coast of Madagascar toward the south, opposite to the dominant winds. The warm water surface signature of the SMACC extends from 22°S (upstream) to 26.4°S (downstream). The SMACC exhibits a seasonal variability: more intense in summer and reduced in winter. The average volume transport of its core is about 1.3 Sv with a mean summer maximum of 2.1 Sv. It is forced by a strong cyclonic wind stress curl associated with the bending of the trade winds along the southern tip of Madagascar. The SMACC directly influences the coastal upwelling regions south of Madagascar. Its existence is likely to influence local fisheries and larval transport patterns, as well as the connectivity with the Agulhas Current, affecting the returning branch of the global overturning circulation.

**Plain Language Summary** A new coastal current: the Southwest Madagascar Coastal Current (SMACC) has been uncovered. This coastal current flows along the southwestern coast of Madagascar toward the south. The SMACC is a relatively shallow (<300 m) and narrow (<100 km wide) warm and salty surface current, which is more intense in summer and reduced in winter. The Southwest Madagascar Coastal Current has a downstream impact on the upwelling system at the south of Madagascar which is a physical process inducing local fertilization. As such, the Southwest Madagascar Coastal Current has key implications for studies about the greater Agulhas Current system, remote connections between oceanographic systems, biophysical coupling in upwelling systems, fisheries management, local livelihoods, and so forth. The uncovering of the SMACC has significant implications for the improved broader understanding of ocean systems around the world.

## 1. Introduction

The ocean circulation in the southwestern Indian Ocean plays an important role in the return loop of the global overturning circulation (Gordon & Fine, 1996; Talley, 2013). In the southwest Indian Ocean, the South Equatorial Current separates in two branches against the east coast of Madagascar (de Ruijter et al., 2004). The northward branch, the North Madagascar Current, bifurcates again along the African continent and forms a poleward flow in the Mozambique channel dominated by large anticyclonic rings (Ullgren et al., 2012), with an estimated mean southward transport of 14 Sv (de Ruijter et al., 2002). The southward branch becomes the East Madagascar Current (EMC), transporting 20 Sv southward along the southeast coast of Madagascar until the southern tip of the island (Ponsoni et al., 2016). Both southward flows are feeding the Agulhas Current system, contributing to the global overturning circulation. The oceanic circulation around Madagascar is currently not completely understood due to limited oceanographic campaigns and ocean dynamics studies. In a recent investigation of the upwelling structure at the southern tip of Madagascar, Ramanantsoa et al. (2018) reported that a significant amount of upwelled waters were not directly coming from the EMC but from the Mozambique Channel, following an alongshore poleward path at the southwest of Madagascar. This could be explained by the presence of a mean poleward warm surface current along the southwest coast of Madagascar, investigated in the present study.

Surface poleward flows along the west coasts of continents are rare in the subtropical latitudes. These include the Leeuwin current, the Navidad current, and the Davidson current. The Leeuwin current is a permanent warm poleward flow along the west coast of Australia (Cresswell & Golding, 1980) with a mean transport of 3.4 Sv (Feng et al., 2003). It flows against strong southerly winds, which regulate its seasonal intensities with a minimum transport in February and a maximum in June (Furue et al., 2017). The Leeuwin current also exhibits an interannual variability associated with El Niño–Southern Oscillation (Furue et al., 2017). The Navidad current is a nonpermanent warm surface current flowing northward, parallel to the shelves of Portugal and northwest Spain, and often observed during the Christmas period (Le Hénaff et al., 2011). The Davidson current is also a nonpermanent poleward surface current which is part of the California Current System along the west coast of North America (Lynn & Simpson, 1987). Throughout fall and winter, the Davidson current develops as a coastal countercurrent (Lynn & Simpson, 1987).

In comparison to these well-documented currents, no studies have as yet revealed the existence of a poleward flow along the west coast of Madagascar in the different sketches of the surface circulation of the Indian Ocean (Schott & McCreary, 2001; Schott et al., 2002, 2009). Tomczak and Godfrey (2003) even report possible events of an equatorward continuation of the EMC along the western flank of Madagascar (see their Figure 11.10). The only hint of a mean surface poleward flow west of Madagascar is that inferred from the dynamic topography map and model velocities at 46 m presented by Schott et al. (2009) (see their Figures 5a and 5b).

Here using in situ and satellite observations as well as model data analyses, we show that a mean poleward warm surface current is present along the southwest coast of Madagascar: the Southwest Madagascar Coastal Current (SMACC). Then, we investigate the spatial extent, transport pathways, and variability of the SMACC, and the mechanism responsible for its occurrence. The outline of the paper is organized as follows: Section 2 details all data sets, model setup, and methods used; section 3 presents the results. Lastly, section 4 provides an interpretation of the findings and summarizes the main results.

## 2. Data, Model, and Methods

SADCP (Shipboard Acoustics Doppler Current Profiler) current measurements were collected during four consecutive years of research cruises between 2007 and 2010 in the Mozambique Channel. SADCP data are used to confirm the direction and intensity of the flow southwest of Madagascar. Conductivity, temperature, and depth profiles, collected from cruises, are also used to identify which water masses make up the SMACC. Details of cruise tracks are given in the supporting information (Table S1).

The Multi-Scale Ultra-High Resolution sea surface temperature (SST), provided on a 0.011° spatial grid (Vazquez-Cuervo et al., 2013), is used to determine the surface signature of the SMACC.

The surface displacements from the Argo-Based Deep Displacement Dataset (Ollitraul & Rannou, 2013), averaged over 2° bins to retain enough observations, are used to compute mean surface velocities.

Trajectories of all available surface drifters encountered southwest of Madagascar are collected from the Global Drifter Programme database ([http://www.aoml.noaa.gov/envids/gld/krig/parttrk\\_id\\_temporal.php](http://www.aoml.noaa.gov/envids/gld/krig/parttrk_id_temporal.php)).

We used the outputs of a two-way nested configuration of the Coastal and Regional Ocean Community model (CROCO) (Debreu et al., 2012; Shchepetkin & McWilliams, 2005). The model was run over 1993–2014 and has a  $\frac{1}{12}$  degree horizontal resolution. The model surface conditions are derived from the European atmospheric reanalysis (ERA-Interim) (Dee et al., 2011). The lateral boundary conditions are forced by the Mercator global ocean reanalysis (GLORYS) (Ferry et al., 2012). A complete description and evaluation of the configuration are given by Ramanantsoa et al. (2018). Lagrangian simulations are also undertaken to advect water parcels following the code described in Gula et al. (2014).

We tested the influence of the wind stress curl on the mean poleward flow using a Sverdrup relation (Sverdrup, 1947) forced by the SCOW climatology of wind stress curl (Risien & Chelton, 2008), as expressed here below:

$$v = \frac{\mathbf{k} \cdot \nabla \times \tau}{H_0 \beta \rho_0} \quad (1)$$

where  $v$  is the meridional velocity in a surface layer of depth  $H_0$  (m),  $\mathbf{k}$  is the unit vector in the vertical direction,  $\beta$  is the meridional gradient of the Coriolis parameter,  $\rho_0$  is the mean water density ( $1,025 \text{ kg m}^{-3}$ ), and  $\tau$  ( $\text{N m}^{-2}$ ) is the wind stress. Results are compared with the mean circulation computed from the Coastal and Regional Ocean Community model outputs averaged over the same depth ( $H_0$ ).

### 3. Results

#### 3.1. Horizontal Structure of the SMACC

A significant amount of upwelled water south of Madagascar is coming from the Mozambique Channel (Figure 1a). This is illustrated by backtracking Lagrangian particles using velocities from the model outputs. Particles are released inside the western upwelling core (black box in Figure 1a) during the maximum upwelling season in austral winter. One hundred twenty-six particles are seeded every 5 m in the upper 50 m and are advected backward in time for 2 months. Over the 2003 to 2013 period, 81% of particles followed consistent pathways along the southwest coast of Madagascar before reaching the upwelling cell, while 19% arrived from the EMC (Figure S1 in the supporting information). This suggests the presence of a mean poleward current along the southwest coast of Madagascar, the SMACC.

The SMACC is present in the model and observations (Figures 1c and 1d). Its signature is visible in SST as a warm tongue of water extending southward along the coast. The warm tongue starts in the vicinity of 22°S in the north and extends southward to 25.5°S. The average surface temperature of this warm flow ranges from 27.2°C upstream to 25.1°C downstream. This water appears to originate from the warm surface waters present in the Mozambique Channel farther north (Halo et al., 2014). The downstream temperature is cooler, probably as a result of air sea interactions and/or mixing with colder upwelled coastal water and waters pumped by cyclonic eddies south of Madagascar (Ridderinkhof et al., 2013).

Mean observed currents derived from the Argo floats surface displacement (Argo-Based Deep Displacement Dataset) (Ollitrault & Rannou, 2013) show a clear alongshore southward flow toward the southern tip of Madagascar. Trajectories of all available drifters extracted from the Global Drifter Programme database (Lumpkin & Pazos, 2007) passing in the region of the SMACC also show directions and pathways consistent with the presence of the SMACC (Figure 1b). Chronologies of these drifters are recapitulated in Table S2 (supporting information). Mean geostrophic currents derived from different mean dynamic topography products also hint to the presence of the SMACC (supporting information Figure S2), albeit with differences in their representation of the current close to the coast. The model highlights a contribution to the SMACC coming from the north (Figure 1c), which is less evident in observations. This difference can also be noticed in the model SSTs (Figure 1c) which are slightly higher than remotely sensed SSTs between 19°S and 22°S (Figure 1d). However, both model and satellite observations are in agreement from 22°S to 25°S and show an alongshore propagation of the SMACC. The SMACC has averaged surface speeds between 20 cm s<sup>-1</sup> and 30 cm s<sup>-1</sup>. Based on the warm tongue and currents vectors plotted in Figures 1c and 1d, the SMACC is approximately 500 km long with a width less than 100 km.

The presence of the SMACC is confirmed by the near-surface current measurements collected from SADCPs at 20 m depth (uppermost data measured) during different cruises (Figure 2). The first two SADCP transects *a* and *b* were made in 2007 and indicate a broad southward surface current. The sea surface height contours taken at the same time show that the strong southward currents visible offshore (more than 50 km from the shelf) at transects *a* and *b* are due to the presence of a cyclone on the west and an anticyclone on the southeast. A local jet-like signature corresponding to the SMACC can be seen off the shelf edge within 50 km from the coast (see red arrows in Figure 2). Geostrophic velocities derived from the sea surface height of Figure 2 do not show any current close to the coast (not shown). The SADCP transect *c* was collected in 2008 (Figure 2). Transect *c* also depicts a southward flow off the shelf edge. The velocity maximum about 80 km away from the shelf corresponds to the currents associated with a cyclonic eddy. The signature of the SMACC is visible as a weaker southward flow ( $\approx 15$  cm s<sup>-1</sup>) over the shelf. The SADCP transects *d*, *e*, *f*, and *g* were made in 2009. They show a southward flow within 50 km from the coast with an averaged velocity of 30 cm s<sup>-1</sup>. While these SADCP sections only provide a few snapshots of the circulation, which do not necessarily correspond to the mean circulation, they still provide growing evidence of the existence of the SMACC.

#### 3.2. Vertical Structure of the SMACC

Modeled vertical cross sections of the time-averaged flow across transects *d*, *e*, *f*, and *g* are presented in Figure 3 (left column) to characterize the vertical structure of the SMACC. At transect *d* (20.4°S), the SMACC consists in a weak poleward flow extending from the surface to 150 m depth and from the coast to 100 km offshore. Farther south, along transects *e* (22°S) and *f* (23.7°S), the SMACC is deeper with larger velocities. The SMACC is most intense near transect *f*, with velocities reaching 25 cm s<sup>-1</sup>. Between transects *f* and *g*, the SMACC decreases in strength and becomes shallower. Observed vertical structure at transect *e* and *f* (Figure 2)

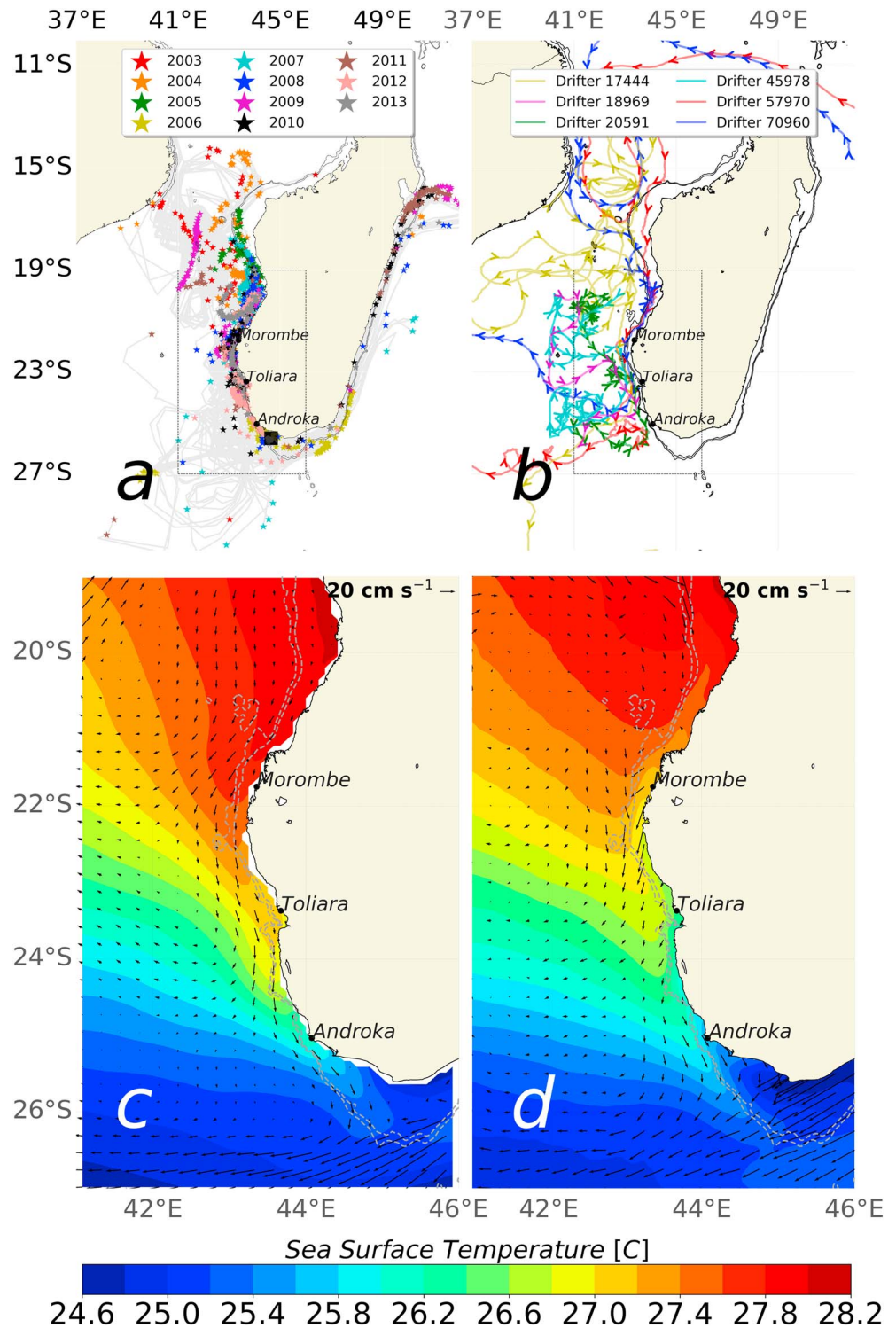


**Figure 1.** (a) Interannual distribution of origin (small stars) and tracks (grey lines) of Lagrangian particles seeded in the upwelling cell south of Madagascar (box in black) and backtracked for 2 months, over the period of 2003–2013. The dotted rectangle shows the region of interest, southwest of Madagascar. Dashed lines show 500 m and 1,000 m isobaths. (b) Trajectories of all available surface drifters within the Global Drifter Programme database (Lumpkin & Pazos, 2007) passing in the southwest of Madagascar. (c) Mean SST and surface currents (arrows) from the model over the period 1993–2013. (d) Mean SST and surface currents (arrows) derived from ANDRO surface displacements covering the period from 1995 to 2016 (Ollivault & Rannou, 2013) (see also Figure S2).

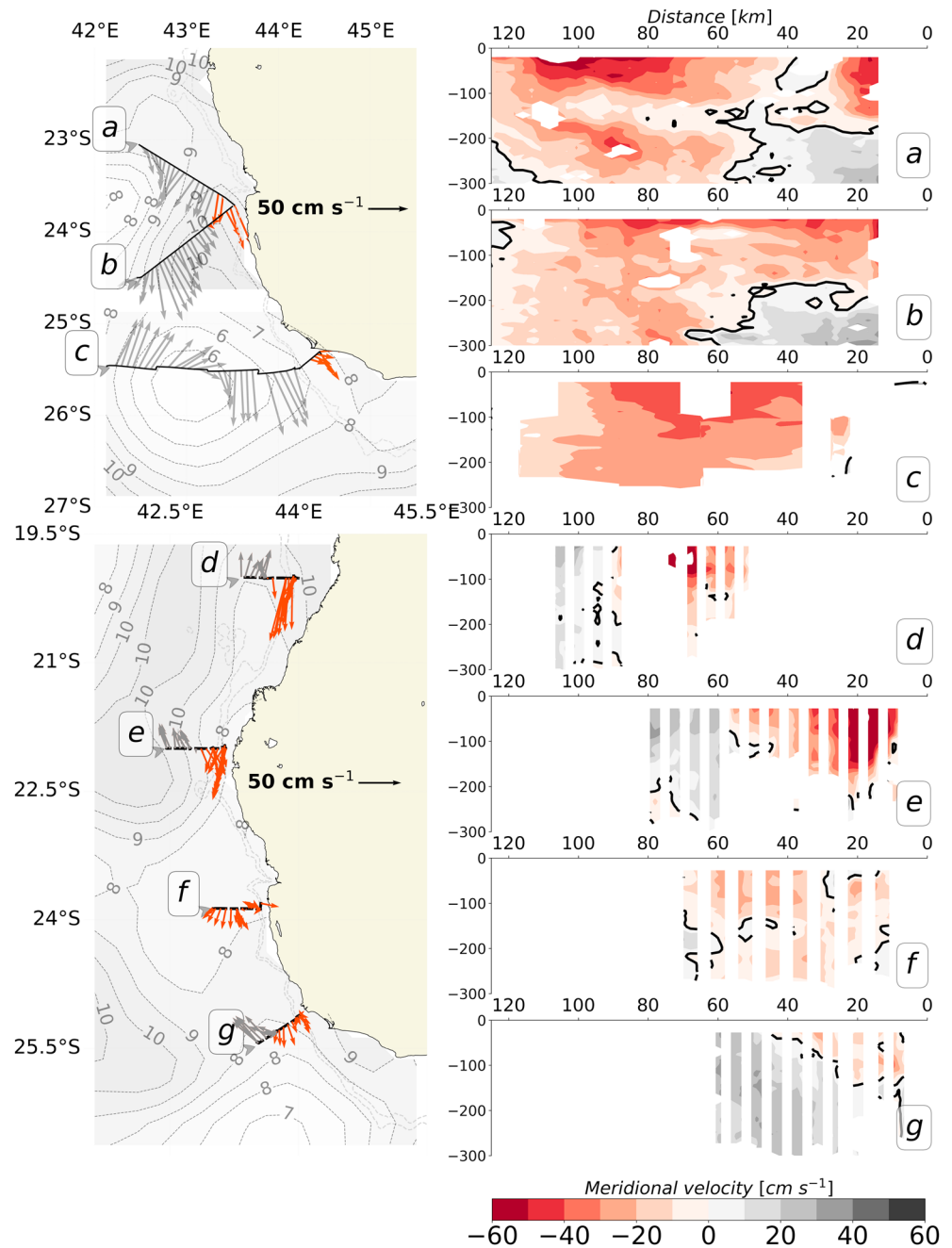


**Figure 2.** (top left column) Transects of Shipboard Acoustics Doppler Current Profiler collected during ACEP 2007 oceanographic cruises (Table S1). Transects *a* and *b* were collected on 13 to 14 September 2007 on board the R/V *Algoa*; *c* was collected on 26–28 September 2008 during ASCLME (Agulhas and Somali Current Large Marine Ecosystem) 2008 cruise on board the R/V *Fridtjof Nansen*. Arrows show the direction and intensities of the measured near-surface currents (20 m) for *a* and *b*, while *c* is represented from the existing data closest to the surface. Red arrows represent the SMACC. Contours depict CLS AVISO (Satellite altimetry data platform) sea surface height for the period of each cruise and at the same date. (bottom left column) Transect *d*, *e*, *f*, and *g* show Shipboard Acoustics Doppler Current Profiler collected during ASCLME 2009 cruise on board the R/V *Fridtjof Nansen* from 26 August 2009 to 4 September 2009 (see Table S1). (right column) Vertical sections of meridional velocities ( $\text{cm s}^{-1}$ ) across the transects. The 0 values are represented by the black contours and the missing values by blank patches. The x axis refers to the offshore distance (km) from the coast.

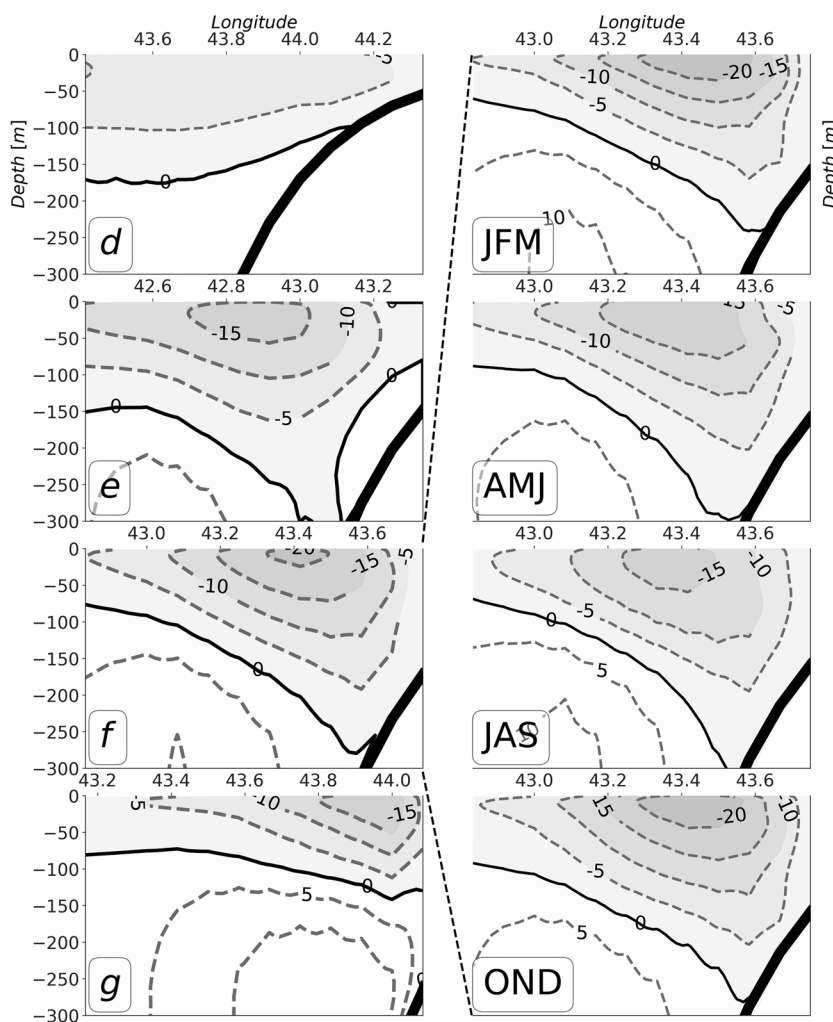


**Figure 3.** (left column) Vertical cross sections of annual mean modeled northward velocities ( $\text{cm s}^{-1}$ ) in the SMACC across transects *d* to *g* shown in Figure 2. Negative speeds indicate a southward flow associated with the Southwest Madagascar Coastal Current. (right column) Seasonal variations of mean northward velocities ( $\text{cm s}^{-1}$ ) across transect *f*. JFM = January to March; AMJ = April to June; JAS = July to September; OND = October to December.

corroborates with the vertical cross sections from the model. At transect *g* the observed flow is weaker and shallower in agreement with the modeled sections. Furthermore, an equatorward undercurrent is visible below the SMACC in the model and observations along this transect (see also supporting information Text S3 and Figure S3).

The location where the SMACC velocities are maximum, near transect *f*, is selected to illustrate seasonal variations in the SMACC meridional velocities (Figure 3). While the width and depth of the SMACC do not significantly change throughout the year, the SMACC is stronger in summer (October to December (OND)-January to March (JFM)) than in winter (April to June (AMJ)-July to September (JAS)). Maximum current velocities in the SMACC of about  $20 \text{ cm s}^{-1}$  and  $25 \text{ cm s}^{-1}$  in OND and JFM are reduced to  $10 \text{ cm s}^{-1}$  and  $15 \text{ cm s}^{-1}$  in AMJ and JAS. The annual volume transport across this transect is  $1.3 \text{ Sv}$  ( $10^6 \text{ m}^3 \text{ s}^{-1}$ ) with seasonal maxima of  $1.6 \text{ Sv}$  and  $2.1 \text{ Sv}$  during the warm season (OND and JFM) and minima of  $0.9 \text{ Sv}$  and  $0.7 \text{ Sv}$  during the cool season (AMJ and JAS). Transports were calculated across Transect *f* (Figure 2), integrated horizontally between  $43^\circ\text{E}$  and  $43.7^\circ\text{E}$  and down to  $250 \text{ m}$  depth. Frequent occurrences of eddies south of Madagascar result in a large variability of the SMACC (Figure 5b), as seen also during the ASCLME 2008 cruise (Figure 2).

Temperature and salinity diagrams (see supporting information Text S4 and Figure S4), from vertical profiles, show that water properties of the SMACC correspond to Subtropical Surface Waters (Donguy & Piton, 1969; Wyrki, 1971; Sætre & Da Silva, 1984).

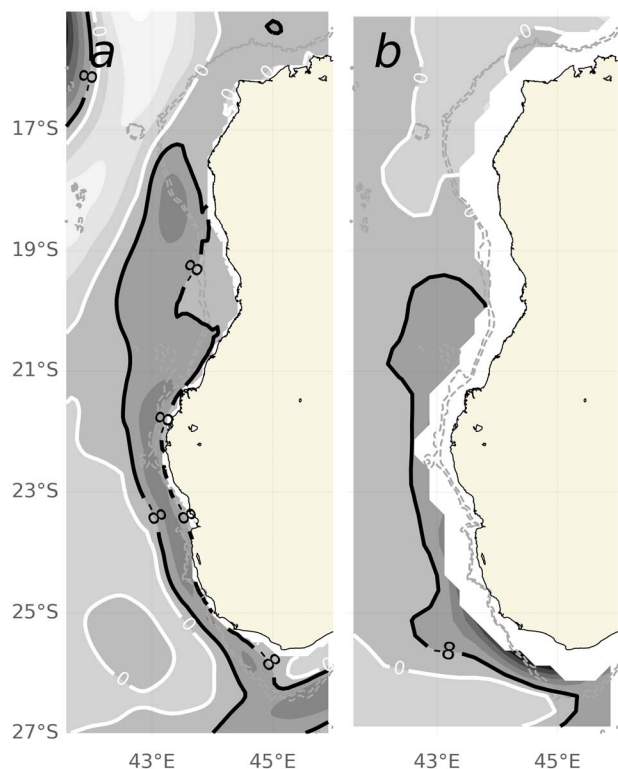


**Figure 4.** Forcing of the Southwest Madagascar Coastal Current: (a) contour plots of meridional velocities averaged over the upper 50 m of the Coastal and Regional Ocean Community model outputs and (b) meridional velocities calculated from the sverdrup relation and using QuikSCAT winds. Labels on the contour line show the magnitude of the meridional velocities in  $\text{cm s}^{-1}$  with darker shades of grey marking regions of increasing meridional velocities.

### 3.3. Forcing of the SMACC

To address the physical process generating the SMACC, we compare mean meridional velocities from the model with predictions from the Sverdrup relation (1) in Figure 4. Both velocities have in common a region of poleward flow along the western Madagascan coastline with meridional velocities higher than  $8 \text{ cm s}^{-1}$ . The lack of QuikSCAT observations near the coast due to land contamination prevents us from computing the Sverdrup circulation there, but the patterns are fairly similar between the model solution and this simple relationship. The bending of the trade winds around the southern tip of Madagascar results in a large cyclonic wind stress curl (especially in January, see the Figure 6 by Risien & Chelton, 2008), forcing a poleward flowing surface current.

## 4. Discussions and Conclusion

Cruise data sets, satellite observations, and analyses of a model output are exploited to reveal the existence of a warm coastal current with a volume transport comparable to that of the Leeuwin current (Furue et al., 2017): the SMACC. The SMACC is a poleward current which flows along the southwestern shores of Madagascar. It flows from  $22^\circ\text{S}$  to the southernmost part of the island near  $26^\circ\text{S}$ . The average length of the SMACC is about 500 km, and its average width is between 50 and 100 km. The SMACC is a warm surface current, which extends over the upper 150 m of the water column upstream and becomes shallower (around 70 m) downstream. The water masses of the SMACC have high salinities characteristic of subtropical surface waters. The average surface speed is around  $20 \text{ cm s}^{-1}$  with an enhancement in the vicinity of Toliara at around  $23.5^\circ\text{S}$  (transect *f* on Figure 3). The average volume transport is 1.3 Sv. The SMACC exhibits a seasonal variability with more intense velocities during the warm season (OND-JFM) and a weakening during the cool season (AMJ-JOS). The mechanism driving the SMACC can be explained by Sverdrup dynamics forced by cyclonic wind stress curl induced

by the bending of the trade winds. The intensity of this surface current is highly related to the magnitude of the winds. The core of the SMACC is intensified at  $24^\circ\text{S}$  due to the enhancement of the wind stress curl south west of Madagascar. In addition, cyclonic eddies generated at the south of Madagascar (Halo et al., 2014) could also contribute to the intensification of the southern part of the SMACC (as seen during the ASCLME 2008 cruise, Figure 2).

The upwelling-related processes in the south of Madagascar are influenced by the SMACC, as highlighted by virtual particles Lagrangian simulations (Figure 1a). Intensification of wind stress curl could also favor the intrusion of the SMACC toward the upwelling system. Ramanantsoa et al. (2018) pointed out that the intrusion of warm waters from the Mozambique Channel could reduce the upwelling surface signature during summer. Figure 5 shows that the annual cycle of the upwelling index defined in (Ramanantsoa et al., 2018) is anticorrelated with the wind stress curl and the SMACC surface speed. This suggests that the intensification of the wind stress curl enhances the SMACC, which brings warm water, reduces the surface signature of the upwelling south of Madagascar, and influences the phytoplankton response associated with the upwelling.

Uncovering the existence of the SMACC brings new understanding for biological and fisheries related management, which is an important socioeconomic component (Bemiasa, 2009; Pripp et al., 2014). Knowledge of the pathway of the SMACC will improve our understanding of the coastal connectivity and lead to better fisheries and ecosystem management. This introduces a prominent process affecting the diffusion and distribution of biological species (shrimp, lobster, small pelagic fish, mangrove, etc.) that will need to be taken into account for the management and emplacement of an eventual marine protected zone.

Zinke et al. (2014) have also addressed the contribution of the southwest of Madagascar waters to the regional circulation. They highlighted a long-term exchange between the southern Mozambique Channel off Toliara

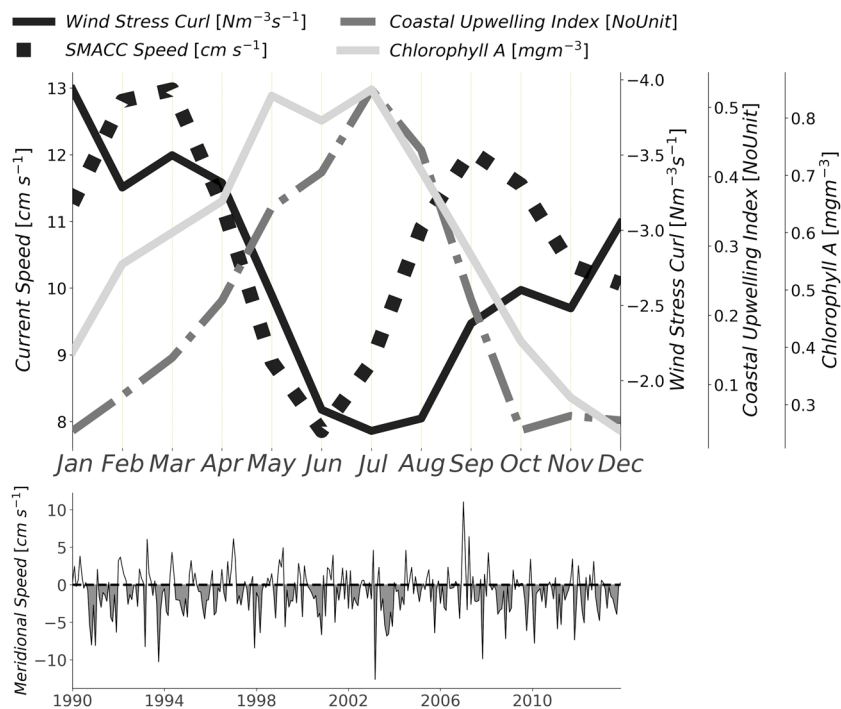


**Figure 5.** (top) Annual variations of wind stress curl ( $\text{N m}^{-3} \text{s}^{-1}$ ) (black solid line), Southwest Madagascar Coastal Current (SMACC)'s surface speed ( $\text{cm s}^{-1}$ ) (dashed black line), coastal upwelling index (dashed grey line), and chlorophyll a concentration ( $\text{mg m}^{-3}$ ) for the upwelling cell. (bottom) Time series of modeled meridional velocities averaged over the first 150 m, representing the SMACC across transect *f*.

(Figure 1) and the Agulhas current core. They found a correlation between coral records and the Agulhas SST reconstruction for the past 334 years, showing a link between the transport of warm water from southwest of Madagascar and the Agulhas current. The SMACC could be instrumental in explaining this link.

#### Acknowledgments

The authors want to thank UCT, CSIR-NRE SRP project ECCCS184, IRD, LOPS, WIOMSA, the NRF SARCHI chair on Ocean Atmosphere Modelling, LMI ICEMASA, the Nansen Tutu for Marine Environmental Research for funding, and RAMI project, a regional doctoral school in the Indian Ocean zone, under the "Horizons Francophones" programme of the AUF (Agence Universitaire de la Francophonie). We thank Marek Ostrowski (IMR Norway), Nansen cruise program, Jean Francois Teron (IRD) and Raymond Roman (UCT) for providing cruise data sets utilized in this study. Numerical computations were performed on the IDRIS (Institut du Développement et des Ressources en Informatique Scientifique) IBM "ADA" computer facility (grant A0020107630) and on the "DATARMOR" computer facility at IFREMER, Brest. The 1992–2002 mean ocean dynamic topography data have been obtained from Nikolai Maximenko (IPRC) and Peter Niiler (SIO). We are grateful to Nicolas Kolodziejczyk for the processing of ANDRO data. The authors are grateful to the anonymous reviewers for their inputs that uplift the quality of this work.

#### References

- Bemiasa, J. (2009). *Dynamique des pêcheries traditionnelles d'anchois, de calmars et de poulpes du sud-ouest de Madagascar: Utilisation d'outils océanographiques pour la gestion des ressources*, (PhD thesis). Université de Toliara, Madagascar.
- Cresswell, G. R., & Golding, T. (1980). Observations of a south-flowing current in the southeastern Indian Ocean. *Deep Sea Research Part A. Oceanographic Research Papers*, 27(6), 449–466. [https://doi.org/10.1016/0198-0149\(80\)90055-2](https://doi.org/10.1016/0198-0149(80)90055-2)
- de Ruijter, W. P., Ridderinkhof, H., Lutjeharms, J. R., Schouten, M. W., & Veth, C. (2002). Observations of the flow in the Mozambique Channel. *Geophysical Research Letters*, 29(10), 1502. <https://doi.org/10.1029/2001GL013714>
- de Ruijter, W. P., van Aken, H. M., Beier, E. J., Lutjeharms, J. R., Matano, R. P., & Schouten, M. W. (2004). Eddies and dipoles around South Madagascar: Formation, pathways and large-scale impact. *Deep Sea Research Part I: Oceanographic Research Papers*, 51(3), 383–400. <https://doi.org/10.1016/j.dsr.2003.10.011>
- Debreu, L., Marchesiello, P., Penven, P., & Cambon, G. (2012). Two-way nesting in split-explicit ocean models: Algorithms, implementation and validation. *Ocean Modelling*, 49, 1–21. <https://doi.org/10.1016/j.ocemod.2012.03.003>
- Dee, D., Uppala, S., Simmons, A., Berrisford, P., Poli, P., Kobayashi, S., ... Vitart, F. (2011). The ERA-Interim reanalysis: Configuration and performance of the data assimilation system. *Quarterly Journal of the Royal Meteorological Society*, 137(656), 553–597. <https://doi.org/10.1002/qj.828>
- Donguy, J.-R., & Piton, B. (1969). Aperçu des conditions hydrologiques de la partie nord du canal de mozambique. *Cahiers ORSTOM.Série Océanographie*, 7(2), 3–26. agris.fao.org.
- Feng, M., Meyers, G., Pearce, A., & Wijffels, S. (2003). Annual and interannual variations of the Leeuwin Current at 32°S. *Journal of Geophysical Research*, 108(C11), 3355. <https://doi.org/10.1029/2002JC001763>
- Ferry, N., Parent, L., Garric, G., Bricaud, C., Testut, C., Le Galloudec, O., ... Zawadzki, L. (2012). Glorys2v1 global ocean reanalysis of the altimetric era (1992–2009) at meso-scale. *Mercator Ocean-Quarterly Newsletter*, 44(2012), 29–39.
- Furue, R., Guerreiro, K., Phillips, H. E., McCreary, J. P., Jr., & Bindoff, N. L. (2017). On the Leeuwin Current System and its linkage to zonal flows in the south Indian Ocean as inferred from a gridded hydrography. *Journal of Physical Oceanography*, 47(3), 583–602. <https://doi.org/10.1175/JPO-D-16-0170.1>
- Gordon, A. L., & Fine, R. A. (1996). Pathways of water between the Pacific and Indian Oceans in the Indonesian seas. *Nature*, 379(6561), 146–149. <https://doi.org/10.1038/379146a0>
- Gula, J., Molemaker, M. J., & McWilliams, J. C. (2014). Submesoscale cold filaments in the Gulf Stream. *Journal of Physical Oceanography*, 44(10), 2617–2643. <https://doi.org/10.1175/JPO-D-14-0029.1>
- Halo, I., Backeberg, B., Penven, P., Ansong, I., Reason, C., & Ullgren, J. (2014). Eddy properties in the Mozambique Channel: A comparison between observations and two numerical ocean circulation models. *Deep Sea Research Part II: Topical Studies in Oceanography*, 100, 38–53. <https://doi.org/10.1016/j.dsr2.2013.10.015>



- Le Hénaff, M., Roblou, L., & Bouffard, J. (2011). Characterizing the Navidad current interannual variability using coastal altimetry. *Ocean Dynamics*, 61(4), 425–437. <https://doi.org/10.1007/s10236-010-0360-9>
- Lumpkin, R., & Pazos, M. (2007). Measuring surface currents with surface velocity program drifters: The instrument, its data, and some recent results. In *Lagrangian analysis and prediction of coastal and ocean dynamics* (pp. 39–67). United Kingdom, UK: Cambridge University Press. <https://doi.org/10.1002/jgrc.20210>
- Lynn, R. J., & Simpson, J. J. (1987). The California Current System: The seasonal variability of its physical characteristics. *Journal of Geophysical Research*, 92(C12), 12,947–12,966. <https://doi.org/10.1029/JC092iC12p12947>
- Ollitrault, M., & Rannou, J.-P. (2013). ANDRO: An argo-based deep displacement dataset. *Journal of Atmospheric and Oceanic Technology*, 30(4), 759–788. <https://doi.org/10.1175/JTECH-D-12-00073.1>
- Ponsoni, L., Aguiar-González, B., Ridderinkhof, H., & Maas, L. R. (2016). The East Madagascar Current: Volume transport and variability based on long-term observations. *Journal of Physical Oceanography*, 46(4), 1045–1065. <https://doi.org/10.1175/JPO-D-15-0154.1>
- Pripp, T., Gammelsrød, T., & Krakstad, J. (2014). Physical influence on biological production along the western shelf of Madagascar. *Deep Sea Research Part II: Topical Studies in Oceanography*, 100, 174–183. <https://doi.org/10.1016/j.dsr2.2013.10.025>
- Ramanantsoa, J. D., Krug, M., Penven, P., Rouault, M., & Gula, J. (2018). Coastal upwelling south of Madagascar: Temporal and spatial variability. *Journal of Marine Systems*, 178, 29–37. <https://doi.org/10.1016/j.jmarsys.2017.10.005>
- Ridderinkhof, W., Le Bars, D., Heydt, A., & Ruijter, W. (2013). Dipoles of the south east Madagascar current. *Geophysical Research Letters*, 40, 558–562. <https://doi.org/10.1002/grl.50157>
- Risien, C. M., & Chelton, D. B. (2008). A global climatology of surface wind and wind stress fields from eight years of QuikSCAT scatterometer data. *Journal of Physical Oceanography*, 38(11), 2379–2413. <https://doi.org/10.1175/2008JPO3881.1>
- Sætre, R., & Da Silva, A. J. (1984). The circulation of the Mozambique Channel. *Deep Sea Research Part A: Oceanographic Research Papers*, 31(5), 485–508. [https://doi.org/10.1016/0198-0149\(84\)90098-0](https://doi.org/10.1016/0198-0149(84)90098-0)
- Schott, F. A., & McCreary, J. P. (2001). The monsoon circulation of the Indian Ocean. *Progress in Oceanography*, 51(1), 1–123. [https://doi.org/10.1016/S0079-6611\(01\)00083-0](https://doi.org/10.1016/S0079-6611(01)00083-0)
- Schott, F. A., Dengler, M., & Schoenefeldt, R. (2002). The shallow overturning circulation of the Indian Ocean. *Progress in Oceanography*, 53(1), 57–103. [https://doi.org/10.1016/S0079-6611\(02\)00039-3](https://doi.org/10.1016/S0079-6611(02)00039-3)
- Schott, F. A., Xie, S.-P., & McCreary, J. P. (2009). Indian Ocean circulation and climate variability. *Reviews of Geophysics*, 47, RG1002. <https://doi.org/10.1029/2007RG000245>
- Shchepetkin, A. F., & McWilliams, J. C. (2005). The Regional Oceanic Modeling System (ROMS): A split-explicit, free-surface, topography-following-coordinate oceanic model. *Ocean Modelling*, 9(4), 347–404. <https://doi.org/10.1016/j.ocemod.2004.08.002>
- Sverdrup, H. U. (1947). Wind-driven currents in a baroclinic ocean; with application to the Equatorial Currents of the eastern Pacific. *Proceedings of the National Academy of Sciences of the United States of America*, 33(11), 318–326.
- Talley, L. D. (2013). Closure of the global overturning circulation through the Indian, Pacific, and southern oceans: Schematics and transports. *Oceanography Society*, 26(1), 80–97.
- Tomczak, M., & Godfrey, J. S. (2003). *Regional oceanography: An introduction* (2nd ed.). New York: Pergamon Press.
- Ullgren, J., van Aken, H., Ridderinkhof, H., & de Ruijter, W. (2012). The hydrography of the Mozambique Channel from six years of continuous temperature, salinity, and velocity observations. *Deep Sea Research Part I: Oceanographic Research Papers*, 69, 36–50.
- Vazquez-Cuervo, J., Dewitte, B., Chin, T. M., Armstrong, E. M., Purca, S., & Alburquerque, E. (2013). An analysis of SST gradients off the Peruvian Coast: The impact of going to higher resolution. *Remote Sensing of Environment*, 131, 76–84. <https://doi.org/10.1016/j.rse.2012.12.010>
- Wyrtki, K. (1971). *Oceanographic atlas of the international Indian Ocean expedition* (Tech. Rep. NSF 86–00-001). Washington, DC: National Science Foundation Publication, OCE.
- Zinke, J., Loveday, B., Reason, C., Dullo, W.-C., & Kroon, D. (2014). Madagascar corals track sea surface temperature variability in the Agulhas Current core region over the past 334 years. *Scientific Reports*, 4, 4393. <https://doi.org/10.1038/srep04393>